

# Unusual $C_{2h}$ -symmetric *trans*-1-(bis-pyrrolidine)-tetra-malonate hexa-adducts of $C_{60}$ . The unexpected regio- and stereo-control mediated by malonate-pyrrolidine interaction.

Edison Castro,<sup>[a]</sup> Khalid Azmani,<sup>[b]</sup> Andrea Hernandez Garcia,<sup>[a]</sup> Amineh Aghabali,<sup>[c]</sup> Shuming Liu,<sup>[a]</sup> Alejandro J. Metta-Magana,<sup>[a]</sup> Marilyn M. Olmstead,<sup>[c]\*</sup> Antonio Rodríguez-Fortea,<sup>[b]</sup> Josep M. Poblet<sup>[b]\*</sup> and Luis Echegoyen.<sup>[a]\*</sup>

**Abstract:** A totally unanticipated regio- and stereo-isomerically pure  $C_{2h}$ -symmetric *trans*-1-(bis-pyrrolidine)-tetra-malonate hexa-adduct of  $C_{60}$  was obtained via a topologically controlled method, followed by a 1,3-dipolar cycloaddition reaction. The structures of the products were elucidated by  $^1\text{H}$ - and  $^{13}\text{C}$ -NMR and by X-ray crystallography. The unexpected regio- and stereo-selectivity supported by theoretical calculations, was found to be mediated by the malonate-pyrrolidine interaction.

## Introduction

The chemical and physical properties of fullerenes and their derivatives are mainly the result of their unique electron accepting abilities and high charge transport capabilities in three dimensions.<sup>[1]</sup> The presence of thirty equivalent [6,6] double bonds on the  $C_{60}$  carbon cage, all of which exhibit identical reactivity, results in low regioselectivity of multiple addition products. After monoadduct formation, subsequent additions of one, two, or three symmetrical addends can yield 8, 46, and 262 possible regioisomers, respectively.<sup>[2, 3]</sup> 1,3-dipolar cycloaddition reactions of azomethine ylides to  $C_{60}$  have been extensively studied and it is one of the most powerful and versatile methods for derivatizing fullerenes.<sup>[4]</sup> Prato and co-workers found that all eight possible *bis*-adduct regioisomers were obtained upon 1,3-dipolar cycloaddition to  $C_{60}$  when the azomethine ylide is symmetric,<sup>[5]</sup> showing that this reaction is less chemoselective than cyclopropanations of  $C_{60}$ .<sup>[6]</sup> The purification of regioisomers by column chromatography is challenging because the *bis*-adducts exhibit similar polarities.<sup>[7]</sup>

There are two well-known methods to reduce the number of regio-isomers of  $C_{60}$  and  $C_{70}$  derivatives, the tether-directed remote multifunctionalization introduced by Diederich *et al.*,<sup>[8]</sup> and the topologically controlled method introduced by Kräutler *et al.*<sup>[9]</sup> Both methods have been widely used to synthesize *bis*, *tris*, *tetra*, *penta* and *hexa*-derivatives of  $C_{60}$ .<sup>[10-12]</sup>

Martin and coworkers reported a straightforward procedure catalyzed by silver or copper acetate to efficiently obtain pyrrolidino[60]fullerenes with stereochemical control by enantioselective cycloaddition of *N*-metalated azomethine ylides to  $C_{60}$ .<sup>[13, 14]</sup> This methodology was later extended to higher fullerenes and endohedral fullerenes.<sup>[15]</sup> Ovchinnikova and coworkers reported an efficient metal-assisted azomethine ylide cycloaddition method for the diastereoselective synthesis of 5-substituted 3,4-fulleroproline esters based on the lithium salt-assisted cycloaddition of azomethine ylides.<sup>[16]</sup> In contrast to the thermal reactions that often result in the formation of diastereomeric mixtures of products, metal-mediated azomethine ylide cycloaddition at low temperature leads to higher yields and diastereoselectivity. However, this kind of reaction has been scarcely studied.

Here, we report a regio- and stereo-selective synthesis of hybrid fullerene  $C_{60}$  hexa-adducts using a combination of an addition and retro addition Diels-Alder reaction, followed by an addition-elimination of bromoethylmalonate, and finally by 1,3-dipolar cycloaddition reactions of azomethine ylides. Surprisingly, only one regio- and stereo-selective product that corresponded to the isomer *cis-anti-cis* hexa-adduct (see Figure 2b for structural nomenclature) was observed. The final products were fully characterized by matrix assisted laser desorption/ionization time-of-flight mass spectroscopy (MALDI-TOF-MS),  $^1\text{H}$  and  $^{13}\text{C}$ -NMR spectroscopy and X-ray crystallography for two of them (*penta* and *hexa*-adduct derivatives). The regio- and stereo-selectivity observed for these two different reactions was supported by theoretical calculations.

<sup>a</sup> Edison Castro, Andrea Hernandez Garcia, Dr. Shuming Liu, Dr. Alejandro J. Metta-Magana and Prof. Dr. Luis Echegoyen, Department of Chemistry, University of Texas at El Paso, 500W University Avenue, El Paso, Texas, 79902, United States, E-mail: echegoyen@utep.edu

<sup>b</sup> Khalid Azmani, Dr. Antonio Rodríguez-Fortea, Prof. Dr. Josep M. Poblet, Departament de Química Física i Inorgànica, Universitat Rovira i Virgili, C/Marcel·lí Domingo 1, 43007 Tarragona, Spain.

<sup>c</sup> Amineh Aghabali, Prof. Dr. Marilyn M. Olmstead, Department of Chemistry, University of California at Davis, One Shields Ave, Davis, California, 95616, United States.

Electronic Supplementary Information (ESI) available: [Experimental and characterization details]. See DOI: 10.1039/x0xx00000x

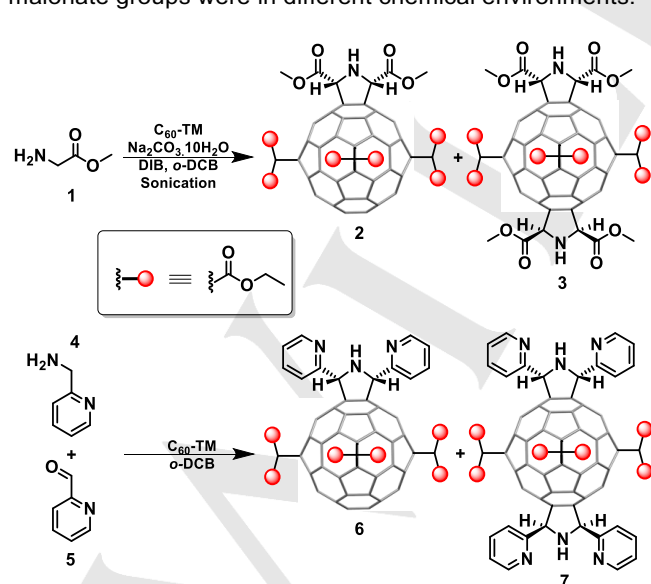
## Results and Discussion

Synthesis and NMR studies of **2**, **3**, **6** and **7**

The  $C_{60}$ -(*e,e,e,e*)-*tetra*-malonate ( $C_{60}$ -TM) (Figure 1a) was synthesized following a procedure previously reported.<sup>[17]</sup> *Penta*-adduct **2** and *hexa*-adduct **3** were synthesized by reacting  $C_{60}$ -TM with methyl glycine ester in the presence of diacetoxyiodobenzene (DIB) and sodium carbonate decahydrate in *ortho*-dichlorobenzene (*o*-DCB) under sonication at room temperature as shown in scheme 1. After 30 min the solution turned orange and compound **2** was the major product, however after 3 h the solution turned yellow and compound **3** was the main product as monitored by TLC using a dichloromethane:ethyl acetate (DCM:EA) 30:1 mixture as the eluent. After column chromatography purification compounds **2** and **3** were characterized by MALDI-TOF-MS and NMR spectroscopy.

The molecular-ion peaks for the *penta*- and *hexa*-adduct compounds at  $m/z$  1511.282 and 1670.341, respectively (Figure S1), were confirmed by MALDI-TOF-MS. Because the azomethine ylide can add to the symmetric or unsymmetric bonds (Figure 1a), two regioisomers are possible. Surprisingly, only one isomer was observed, and by  $^1\text{H}$ - and  $^{13}\text{C}$ -NMR and X-ray crystal structure a  $C_s$  symmetry was assigned to compound **2**.

The  $^1\text{H}$ -NMR spectrum of **2** (Figure 3a) exhibits only one set of signals for the pyrrolidine addend ( $\delta = 4.69, 3.89$  and  $3.76$  ppm), clearly establishing the presence of a plane of symmetry, indicating that the addition must have occurred on the symmetric bond (Figures 1b and 1c). The  $C_s$  symmetry of compound **2** was also confirmed by the  $^{13}\text{C}$ -NMR spectrum (Figure 3b). Five resonances for carbonyl groups at  $\delta = 169.0$  (ester groups of the pyrrolidine addend),  $163.8$  ( $\times 2$ ),  $163.7$  and  $163.4$  ppm (four malonates), five resonances for the methyl groups at  $\delta = 52.9.0$  (methyl groups of the pyrrolidine addend),  $14.2$  ( $\times 2$ ) and  $14.1$  ( $\times 2$ ) ppm (four malonates) indicate that the four malonate groups were in different chemical environments.



**Scheme 1.** Synthesis of *penta*-adducts **2** and **6** and *hexa*-adducts **3** and **7**.

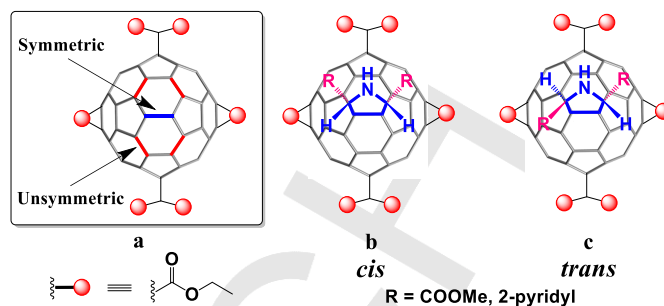


**Figure 1.** a) symmetric and unsymmetric double bonds, b) symmetric *cis* addition, c) symmetric *trans* addition.

Twenty four  $^{13}\text{C}$  resonances between  $\delta = 138.0$  and  $152.2$  ppm were observed for the  $\text{sp}^2$  carbons of the fullerene cage, two resonances at  $\delta = 76.0$  and  $72.1$  ppm from the pyrrolidine ring, and four resonances at  $\delta = 63.1 \times 2, 63.0$  and  $62.7$  ppm assigned to the methylene groups, in agreement with the four resonances expected for the methylene groups.

Finally, the stereospecific *cis*-addition (Figure 1b) was unambiguously established by the six  $\text{sp}^3$  signals observed for the fullerene carbon atoms at  $\delta = 69.9, 69.8, 69.5, 69.3, 45.5$  and  $45.1$  ppm and the three  $\text{sp}^3$  signals for the carbons of the four cyclopropane rings at  $\delta = 67.8, 67.5$  and  $44.8$  ppm (Figure 3b). If the *trans*-addition had occurred (Figure 1c) only four  $\text{sp}^3$  signals for the fullerene carbon atoms and two  $\text{sp}^3$  signals for the cyclopropane rings would have been observed.

To further support the regio- and stereo-chemistry of compound **2**, crystals were grown by slow evaporation in toluene. The results of the X-ray structure determination are shown in figure 7a. The structure not only clearly reveals the *cis* orientation of the pyrrolidine addend but also the addition at the symmetric double bond (Figure 1).

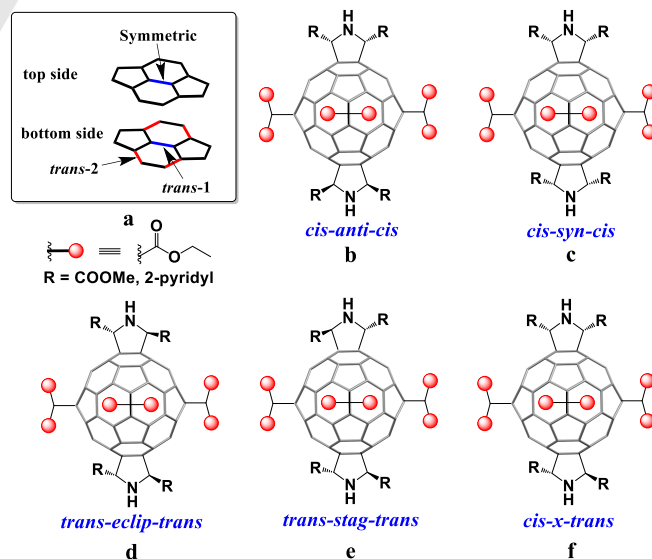


**Figure 2.** Possible *hexa*-adduct stereoisomers of  $C_{60}$  (taking into account only symmetric and *trans-1* additions of azomethine ylide to  $C_{60}$ -TM).

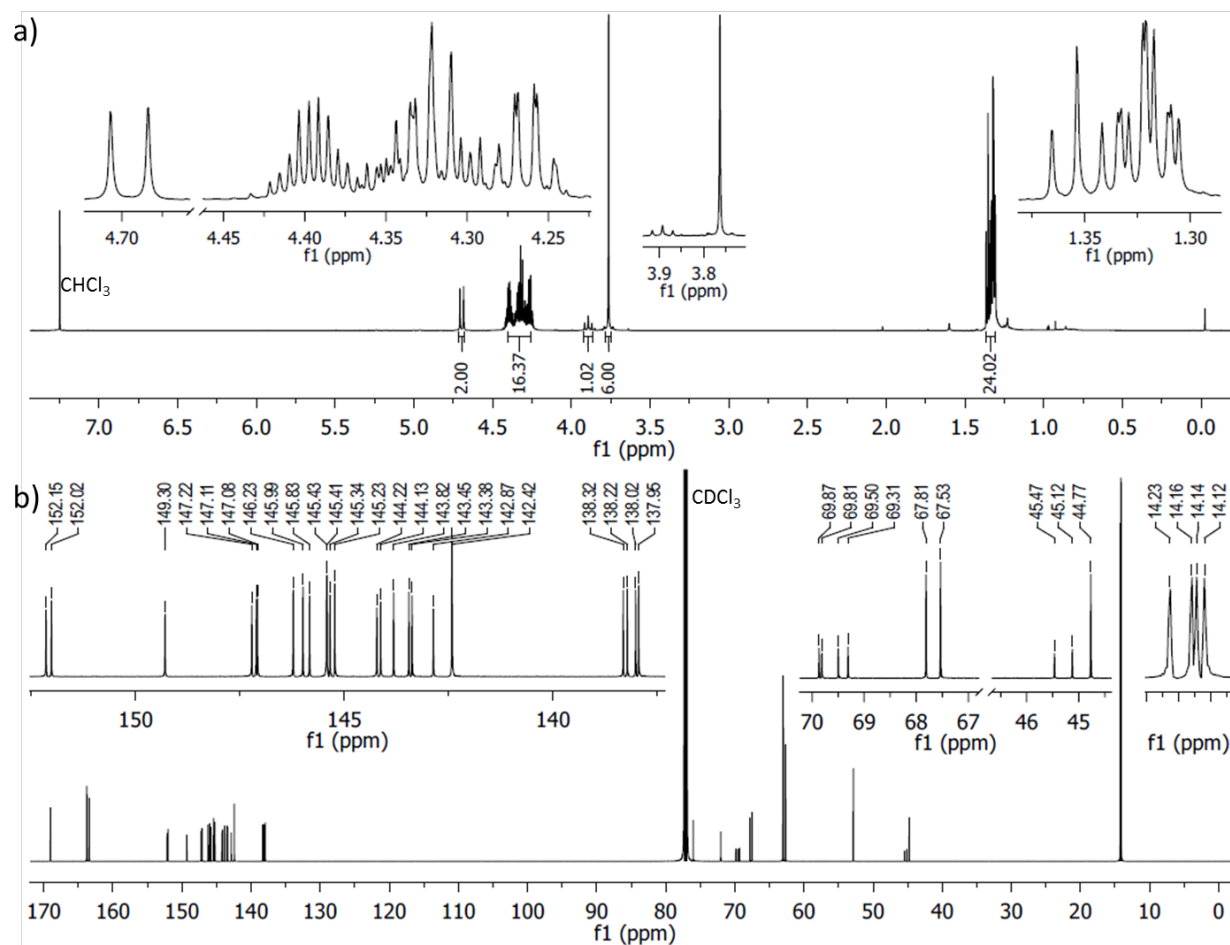


**Figure 3.**  $^1\text{H}$ - and  $^{13}\text{C}$ -NMR of compound **2**, ( $\text{CDCl}_3$ ).

Compound **3** was identified as the *hexa*-adduct with the pyrrolidines in a *trans-1* relative position, as shown in figure 2a. The  $^1\text{H}$ -NMR of compound **3** (Figure 4a) exhibits only one set of signals for the two pyrrolidines ( $\delta = 4.90$ , 3.82 and 3.69 ppm), showing the presence of a plane of symmetry, which is only possible if the second addition occurs on the *trans-1* position. Figures 2b-f represent all the five possibilities for the *trans-1* isomers, where the first and third descriptors refer to the pyrrolidine stereochemistry and the middle one refers to their relative orientation. For example the isomer 2b *cis-anti-cis* refers to the two substituents on the pyrrolidine being in a *cis* position but in *anti* orientation with respect to the other pyrrolidine substituents (Figures 5A and 5B).

The  $^{13}\text{C}$ -NMR spectrum of compound **3** showed twelve resonances for the  $\text{sp}^2$  carbons of the fullerene cage between  $\delta = 152.3$ -139.1 ppm, two resonances for the pyrrolidines at  $\delta = 74.0$  and 72.9 ppm, one resonance for the methoxy groups at  $\delta = 52.8$  ppm, two resonances at  $\delta = 66.4$  and 44.4 ppm for the cyclopropane carbon-bridged atoms, two resonances for the methylene groups and two for the methyl groups of the malonates at  $\delta = 63.0$ , 62.5 and  $\delta = 14.1 \times 2$ , respectively. Surprisingly, only three carbonyl group resonances were observed, one at  $\delta = 169.4$  ppm, assigned to the carbonyl groups of the pyrrolidine addends

and two at  $\delta = 163.5$  and 163.4 ppm, assigned to the carbonyl groups of the four malonates.

These observations are consistent with two structures, one where the pyrrolidines are both *cis* but anti relative to each other (Figure 2b), or one where the groups in the pyrrolidine are *trans* but the two pyrrolidines are staggered (Figure 2e). For structures 2e, 2d and 2f four resonances for the carbonyl groups are expected (one for the carbonyl groups of the pyrrolidines and three for the carbonyl of the malonates).

The  $\text{sp}^3$  resonances from the cyclopropane carbon atoms were crucial to unambiguously identify the structure of compound **3**. Three resonances at  $\delta = 70.9$ , 70.8 and 45.6 ppm clearly prove that the *cis-anti-cis* isomer (Figure 2b) was the product obtained, since only two resonances would be observed for the *trans-stag-trans* isomer, as shown in figure 5.

Based on the surprising and unprecedented regio- and stereo-selectivity observed for compound **3**, we decided to study this reaction using a different substituent (2-pyridyl) on the pyrrolidine addends (compound **7**) as shown in scheme 1.

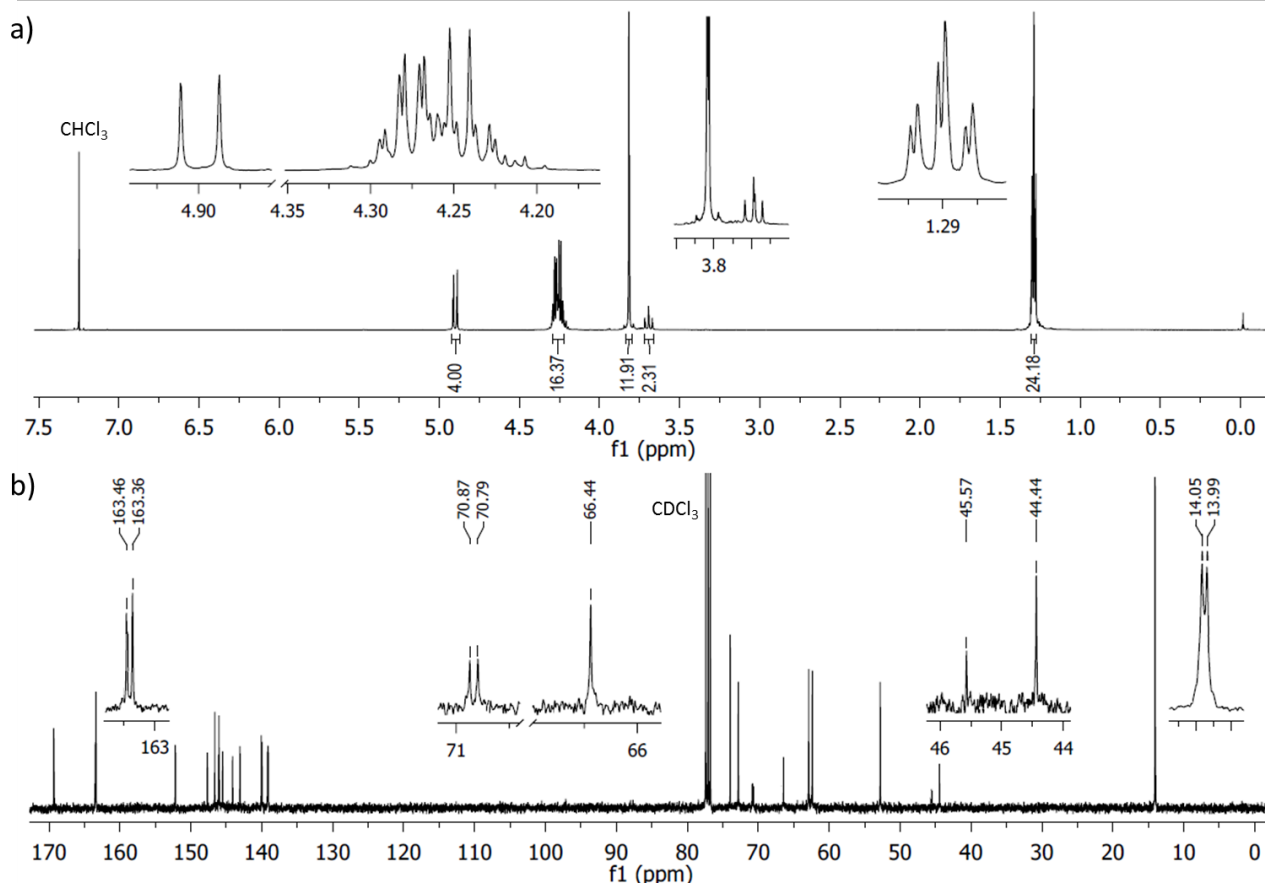


**Figure 4.**  $^1\text{H}$ - and  $^{13}\text{C}$ -NMR of compound **3**, ( $\text{CDCl}_3$ ).

*Hexa*-adduct **7** was synthesized by reacting  $\text{C}_{60}$ -TM with 2-picolylamine (**4**) and 2-pyridinecarbaldehyde (**5**) in *o*-DCB, under reflux for 30 min.

After 30 min the solution turned yellow, and the main product, compound **7**, was purified by silica gel column chromatography using a chloroform:methanol ( $\text{CHCl}_3$ :MeOH) 15:1 mixture. The reaction was monitored by TLC using the same mixture of solvents. The isolated product **7** was characterized by MALDI-TOF-MS and by NMR spectroscopy.

The MALDI-TOF-MS confirmed the presence of the molecular-ion peak for the *hexa*-adduct derivative at  $m/z$  1746.425 (Figure S4). NMR Analysis similar to the one conducted with compound **3** confirmed the regio- and stereo-selectivity of the  $C_{2h}$ -symmetric *trans*-1 addition of compound **7**, as for compound **3**.

The  $^1\text{H}$ -NMR spectrum of compound **7** (Figure S5a) shows a doublet at  $\delta = 5.52$  ppm, which corresponds to the four identical pyrrolidine protons, in the aromatic region four signals were assigned to the 2-pyridyl groups and a triplet at  $\delta = 5.06$  ppm was assigned to the NH of the pyrrolidine addends. One  $\text{ABX}_3$  and one  $\text{AMX}_3$  system were observed for the methylene groups of the four malonates at  $\delta = 4.25$  and 4.12 ppm, respectively (Figure S5a). Two triplets at  $\delta =$

1.28 and 1.22 ppm reflect the different chemical environments of the methyl groups of the four malonates.

The  $^{13}\text{C}$ -NMR spectrum (Figure S5b) of compound **7** showed similar resonances to that of compound **3**. Two resonances for the carbonyl groups at  $\delta = 163.8$  and 163.4 ppm, seventeen resonances between 156.1 and 122.6 ppm (twelve resonances for the  $\text{sp}^2$  fullerene carbon atoms and five for the 2-pyridyl groups), two resonances for the pyrrolidine addends at  $\delta = 70.6$  and 76.5 ppm, two resonances for the methylene groups at  $\delta = 62.7$  and 62.1 ppm, and two resonances for the methyl groups at  $\delta = 14.1$  ppm. Finally, five resonances at  $\delta = 72.7$ , 70.9, 66.2, 45.4 and 44.1 ppm prove the presence of the *cis-anti-cis* isomer.

#### Crystallography studies

The crystal structure of compound **2**, (Figure 7a) clearly shows a plane of symmetry and thus confirming the *cis* orientation of the two substituents (ester groups at C61 and C64) in the pyrrolidine. The C1-C2 (Figure 7a) distance is 1.590(3) Å, longer than the typical 6:6 distance of 1.38 Å in pristine  $\text{C}_{60}$ .

Crystal data for **2**:  $a = 12.9239(7)$ ,  $b = 13.9988(7)$ ,  $c = 20.5853(11)$  Å,  $\alpha = 88.077(2)$ ,  $\beta = 74.686(2)$ ,  $\gamma = 65.018(2)^\circ$ ,  $U = 3243.0(3)$  Å<sup>3</sup>,  $T = 100$  K, red blocks, space group  $P1$  (no. 2),  $Z =$

2, 35340 reflections measured, 14518 unique ( $R_{\text{int}} = 0.031$ ),  $R_1(I > 2\sigma(I)) = 0.0494$ ,  $wR_2(\text{all data}) = 0.1309$ .

We failed in our attempts to grow single crystals of compound **7** using different solvents such as toluene, chloroform and dichloromethane. A variety of functionalized terpyridines have been complexed using different metals including Zn,<sup>[18, 19]</sup> therefore, crystals of compound **7** were grown by complexation with  $\text{ZnBr}_2$  by slow evaporation in a benzene:chloroform:ethanol 9:9:1 mixture (Figure 7b). The X-ray crystallography data shows a discrete molecule where compound **7** was complexed with two molecules of  $\text{ZnBr}_2$ . These results confirm the exclusive observation of the *cis-anti-cis* structure. The crystallographic inversion center found in the structure of **7** confirms that two pyrrolidines are in *trans-1* positions. The pyridyl substituents at C31 and C32 are in *cis* orientation, yet they are *anti* with respect to the other pyrrolidine substituents (Figure 7b).

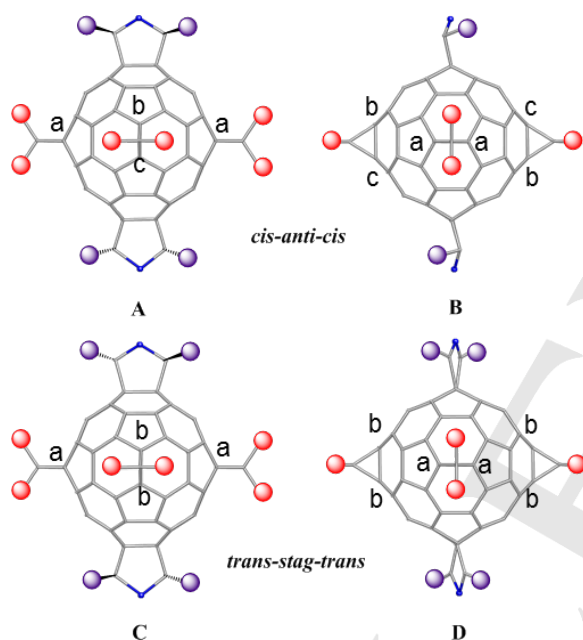


**Figure 5.** Front and side views of the *cis-anti-cis* (A and B) and *trans-stag-trans* (C and D) fullerene *hexa*-adducts. Red balls represent the ethyl carboxylate groups ( $-\text{COOC}_2\text{H}_5$ ) and the purple balls represent either the methyl carboxylate ( $-\text{COOCH}_3$ ) or the 2-pyrrolidine ( $-\text{C}_5\text{H}_4\text{N}$ ).

The coordination geometry at Zn1 is intermediate between trigonal bipyramidal and square pyramidal. The pyrrolidine attachment length at the C1-C2 (Figure 7b) 6:6 bond distance is 1.587(5) Å. Crystal data for **7**:  $a = 14.8721(7)$ ,  $b = 13.3913(7)$ ,  $c = 27.1851(12)$  Å,  $\beta = 104.206(3)^\circ$ ,  $U = 5248.5(4)$  Å<sup>3</sup>,  $T = 100$  K, yellow needles, space group  $P2_1/n$  (no. 14),  $Z = 2$ , 72431 reflections measured, 12022 unique ( $R_{\text{int}} = 0.083$ ),  $R_1(I > 2\sigma(I)) = 0.0604$ ,  $wR_2(\text{all data}) = 0.1597$ .

Details of the solution and refinement of the structures are available in the crystallographic information files (CIF).

### Computational analysis

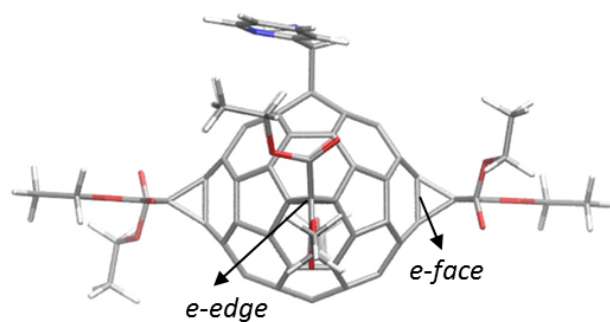
DFT calculations were performed to rationalize the selective formation of the *cis-anti-cis* isomers as shown in scheme 1. To understand the different factors that govern the stereoselectivity for this kind of reactions, the addition of one azomethine ylide to form the *mono*-pyrrolidine *penta*-adduct was initially studied. Afterwards, the possible isomers of the *bis*-pyrrolidine *hexa*-adducts were analyzed.

**The *mono*-pyrrolidine *penta*-adduct.** *Cis* (1b) and *trans* (1c) pyrrolidine groups can result from the conformation of the azomethine ylide, which can exist in a W- or S-shape.<sup>[20]</sup> Cycloadditions of azomethine ylides to C<sub>60</sub> show differences around 1-2 kcal mol<sup>-1</sup> in favor of the *cis* conformation.<sup>[20]</sup>

The slightly higher stability of the *cis* vs the *trans* isomer is mainly due to the deformation degree of the pyrrolidine addend. DFT calculations were carried out to find the reaction energies of the 1,3-dipolar cycloaddition of azomethine ylide to C<sub>60</sub>, *e,e,e,e*-(tetramethylene)-C<sub>60</sub> ((CH<sub>2</sub>)<sub>4</sub>C<sub>60</sub>) and C<sub>60</sub>-TM models. Values in Table 1 show higher reaction energies for C<sub>60</sub>-TM than that of C<sub>60</sub> and (CH<sub>2</sub>)<sub>4</sub>C<sub>60</sub> models. Furthermore, stabilization of the *cis* vs the *trans* conformation is enhanced from energy differences of 1-2 kcal mol<sup>-1</sup> to 2-4 kcal mol<sup>-1</sup>. These results can be explained by the different interactions between the malonate groups and the pyrrolidine addend in each of the two isomers (*vide infra*).

The malonate-pyrrolidine adduct interaction (MAI) was quantified as the difference between the bonding energy (BE) of the pyrrolidine addend (pa) in C<sub>60</sub>-TM and that in the (CH<sub>2</sub>)<sub>4</sub>C<sub>60</sub> model, where the four malonates are replaced by four methylene groups,  $\text{MAI} = \text{BE}[\text{pa}-\text{C}_{60}\text{-TM}] - \text{BE}[\text{pa}-(\text{CH}_2)_4\text{C}_{60}]$ . With this definition, we are assuming that there is no interaction between the pyrrolidine addend and the methylenes within our reference (CH<sub>2</sub>)<sub>4</sub>C<sub>60</sub> model.

The MAI values range between -4 and -6 kcal mol<sup>-1</sup> (see values in Table 1) for the *trans* and *cis* isomers of the ester- and pyridyl-substituted pyrrolidine adducts, meaning that there is a non-negligible attractive interaction between the equatorial malonates and the substituents of the pyrrolidine addend. To verify this result, we have also considered a simplified model system made only by the pyrrolidine and the malonates, without considering the carbon cage (see Figure S7), to compute the interaction energies between these groups (pyrrolidine-malonates) for the *cis* isomers of the ester- and pyridyl-pyrrolidine adducts. The interaction energies thus computed are very similar to the MAI values, confirming the validity of the latter as a measure of such interaction (see values in Table S2).



a)

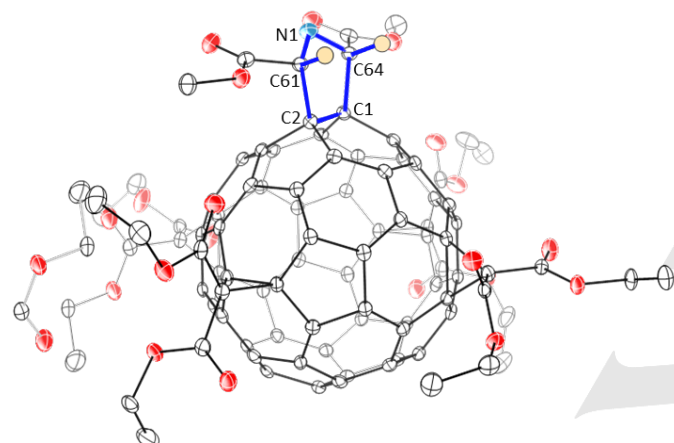


**Figure 6.** Optimized structure of *mono*-(pyridyl-pyrrolidine) *penta*-adduct of  $C_{60}$ .

b)

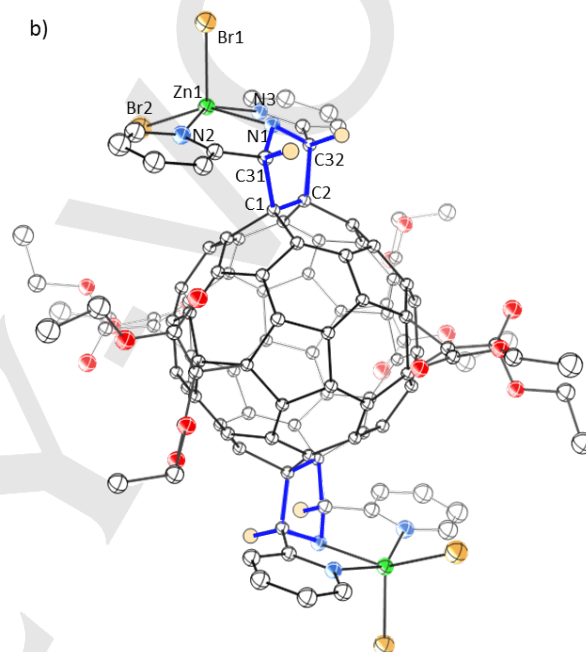


**Figure 7.** Crystal structure of a) compound **2** and b) compound **7** complexed with  $ZnBr_2$ . Atoms labelled C1 and C2 are part of the  $C_{60}$  and are symmetrically placed at a 6:6 junction. Atoms are drawn with thermal ellipsoids at the 50% probability level.

To gain more insight into the nature of the interaction between the pyrrolidine substituents and the malonates, we have performed calculations on some of our fragment models without taking into account the dispersion corrections (see Table S2 and Figure S7). The results, which show positive, i.e. repulsive, interaction energies confirm that the attractive interaction results from dispersion forces between the pendant groups in the malonate and the pyrrolidine.

We have also found that the pyrrolidine-malonates interaction critically depends on the addition position of the malonate chains. There are two types of malonate addends as a result of *e-face* and *e-edge* additions (Figure 6). The *e-edge* malonates, compared to the *e-face* ones, are closer to the pyrrolidine group substituents, thus inducing a significantly larger interaction. Indeed, calculations using a series of pyrrolidino  $C_{60}$ -dimalonate models confirm that the *e-edge* adducts are responsible for the main contribution to

the total pyrrolidine-malonates interaction (Tables S2 and S3).

**Table 1.** Bonding energies (BE, in the gas phase) and MAI values of the *mono*-pyrrolidine adducts (ester and pyridyl-substituted) with  $C_{60}$ ,  $(CH_2)_4C_{60}$  model and  $C_{60}$ -TM.<sup>a</sup>

BE	Ester		Pyridyl	
	<i>cis</i> (1b)	<i>trans</i> (1c)	<i>cis</i> (1b)	<i>trans</i> (1c)
$C_{60}$	-28.8	-27.9	-30.8	-28.8
$(CH_2)_4C_{60}$	-27.2	-26.3	-28.5	-26.4
$C_{60}$ -TM	-31.8	-30.1	-34.2	-30.4
MAI <sup>b</sup>	-4.6	-3.8	-5.7	-4.0

<sup>a</sup> All energy values are expressed in  $\text{kcal mol}^{-1}$ . <sup>b</sup> Malonate-pyrrolidine adduct interaction is calculated as  $MAI = BE[\text{pa-}C_{60}\text{-TM}] - BE[\text{pa-}(CH_2)_4C_{60}]$ .

Calculations were also carried out in *o*-DCB, which was the solvent used in experiments. Both the position and the geometry of the malonate chains were slightly affected by the solvent, therefore the interaction between the malonates and the pyrrolidine groups was also affected. The results still show the stabilization due to the interaction

between the pyrrolidine substituents and the malonates already found in gas phase calculations. Interestingly, a different trend for this interaction was observed depending on the pyrrolidine group substituents. For the ester group, the value of the MAI,  $-2.1 \text{ kcal mol}^{-1}$ , is affected drastically, decreasing by half in comparison with the gas phase value, while for the pyridyl the MAI,  $-5.3 \text{ kcal mol}^{-1}$ , does not change appreciably. These results are related to the free space available between the pyrrolidine group and the malonate chains that can be accessible to solvent molecules. The bulkier and less flexible the pyrrolidine group, the smaller the space for the solvent to access the region in between the malonate and the pyrrolidine, therefore the smaller the change with respect to the MAI in the gas phase. As long as the regions of the malonate and the pyrrolidine that interact through dispersion forces are more effectively solvated, their attractive interactions decrease and the MAI is reduced.

**The bis-pyrrolidine hexa-adduct.** The different stereoisomers resulting from the second 1,3-dipolar cycloaddition on the symmetric bond (Figure 1) can be classified into two sets. On one hand, there are those isomers with two *cis*-pyrrolidine groups (2b and 2c in Figure 2), and on the other, those isomers with at least one *trans* group (2d, 2e and 2f in Figure 2). The *trans* conformation of the pyrrolidine group results in a destabilization of the system with respect to the *cis* one. The second set of isomers, which contains at least one *trans*-pyrrolidine group, is around 3-7  $\text{kcal mol}^{-1}$  higher in energy than the first set (see values in Table 2). In general, the higher the number of *trans* groups, the larger the destabilization. However, the results do not show a strictly additive effect.

Looking at the first set of isomers, the energy differences between the isomers 2b and 2c are rather small. The only difference between these two isomers is the relative position of the two *cis*-pyrrolidine groups, which can be either in *syn* or in *anti* position relative to each other (Figure 2). In the case of the pyridyl-pyrrolidine group, 2c (*syn*) is slightly lower in energy than 2b (*anti*). For the ester-pyrrolidine group, the two isomers are almost degenerate, with 2b (*anti*) being only  $0.2 \text{ kcal mol}^{-1}$  lower in energy than 2c (*syn*). These small differences are a consequence exclusively of the presence of the malonate chains as the same systems without malonates are degenerate (see Table S4). These energy differences are essentially kept when using hybrid functionals (see Table S5).

As for the *mono*-pyrrolidine *penta*-adduct, we calculated the MAI for 2b-2f (see Table 2). The results are around two times those of the *penta*-adduct. For the ester-pyrrolidine *penta*-adduct 1b the MAI is  $-4.6 \text{ kcal mol}^{-1}$  and for the *hexa*-adduct 2b it is  $-8.9 \text{ kcal mol}^{-1}$  (Table 2). Therefore, the MAI value is the result of additive independent interactions for each of the two pyrrolidine adducts with the malonate chains.

As found for the *penta*-adduct, solvent is a crucial factor to compute the malonate-pyrrolidine interaction, which can be seen as the driving force for the formation of these compounds. The solvent affects the malonate chains, and solvates the adducts, reducing the strength of this interaction. Stabilization of the 2b (*anti*) isomer, which is the one obtained experimentally, with respect to 2c (*syn*) is enhanced when *o*-DCB is present. For the ester-pyrrolidine group, an increase of the energy difference between the two isomers is found (from 0.2 to  $0.5 \text{ kcal mol}^{-1}$ ). For the pyridyl-pyrrolidine isomers, an inversion of relative stability is observed (see Table 4). Furthermore, the MAI values are affected by the solvent in the same way as for the *penta*-adduct.

**Table 2.** Binding energies (BE), relative energies ( $\Delta E$ , gas phase and solvent) with MAI values (in parenthesis), free energies and percentage for different  $C_{60}$  hexa-adducts.<sup>a</sup>

Group	Iso	cis/ trans	BE gas	$\Delta E$ gas	$\Delta E$ solv <sup>b</sup>	$\Delta G$ <sup>c</sup>	Iso % <sup>c</sup>
Ester	2b	2/0	-61.4	0.0 (-8.9)	0.0 (-3.4)	0.0	75.8
	2c	2/0	-61.2	0.2 (-8.8)	0.5 (-3.0)	0.9	16.8
	2d	0/2	-59.9	4.5 (-6.3)	3.2 (-2.3)	2.1	2.4
	2e	0/2	-59.0	2.4 (-8.2)	1.1 (-4.2)	2.1	2.3
	2f	1/1	-58.4	3.0 (-6.6)	2.6 (-1.4)	2.0	2.7
Pyridyl	2b	2/0	-63.5	1.1 (-8.9)	0.0 (-7.5)	0.0	98.3
	2c	2/0	-64.6	0.0 (-10.0)	0.7 (-6.8)	2.4	1.7
	2d	0/2	-58.4	6.2 (-8.0)	7.3 (-4.7)	8.2	0.0
	2e	0/2	-57.9	6.8 (-7.5)	6.5 (-5.4)	5.0	0.0
	2f	1/1	-61.0	3.7 (-8.4)	3.2 (-6.6)	4.9	0.0

<sup>a</sup> Energies in  $\text{kcal mol}^{-1}$ ; <sup>b</sup> *o*-DCB; <sup>c</sup> At 300 K

The different interaction with the solvent helps to explain the stabilization of 2b with respect to 2c. The optimized structures show that the malonate chains in 2b are compact and close to the pyrrolidine groups. However, in 2c they tend to be farther from the pyrrolidine groups and thus easier to be solvated, consequently reducing the interaction strength with the pyrrolidine groups (Figure 8). This effect is quite critical for the pyridyl-pyrrolidine derivative where the MAI value for 2b ( $-6.8 \text{ kcal mol}^{-1}$ ) is rather similar to that of the *mono*-pyrrolidine *penta*-adduct ( $-5.3 \text{ kcal mol}^{-1}$ ).

Finally, we have computed the free energies, within the rigid rotor and harmonic oscillator (RRHO) approximation, at the temperature and pressure conditions of the experiment. The results show that isomer 2b is favored with respect to 2c, by up to almost  $1 \text{ kcal mol}^{-1}$  for the ester- and  $2.4 \text{ kcal mol}^{-1}$  for the pyridyl-pyrrolidine. This relative stabilization is governed mainly by the entropic contribution. We have also computed the free energy for the other three isomers 2d, 2e and 2f. For the pyridyl-substituted hexa-adduct, the relative free energies for 2d-2f are rather high compared to 2b (more than  $5 \text{ kcal mol}^{-1}$ , see Table 2). For the ester-substituted hexa-adduct, however, the free energy differences are not so large, in line with their energy differences (see Table 2).

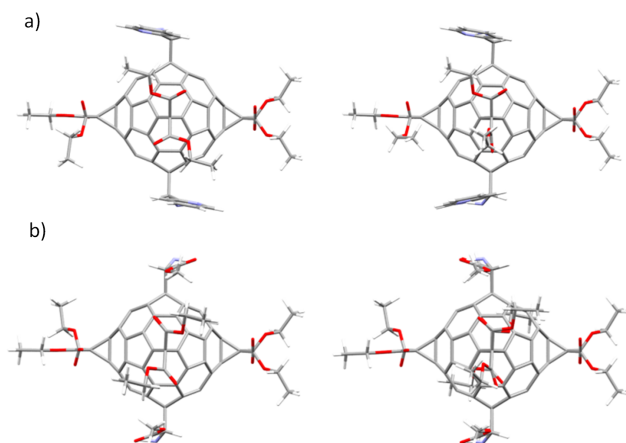


**Figure 8.** Optimized structure in *o*-DCB of anti and syn isomers of a) pyridyl-substituted and b) ester-substituted bis-pyrrolidine hexa-adducts of  $C_{60}$ .

Such differences in the free energies lead to relative abundances for the *cis-anti-cis* (2b) vs *cis-syn-cis* (2c) stereoisomers at experimental conditions of 76% vs 17% for the ester group and 98% vs 2% for the pyridyl group, in good agreement with experiments. The percentages for the rest of isomers 2d-2f are small for the ester group (around 2%) and negligible for the pyridyl group (0%).

## Conclusions

We have synthesized a new hexa-adduct derivative of  $C_{60}$  by a 1,3-dipolar cycloaddition reactions via two different conditions and using  $C_{60}$ -TM as the starting material. These reactions are highly regio- and stereo-selective, leading to the exclusive formation of the *cis-anti-cis* isomer. The formation of the *cis-anti-cis* hexa-adduct isomers as the only observed products was mainly attributed to the interaction between the pendant groups in the malonate and pyrrolidine groups. This interaction, which is very important in the gas phase (van der Waals type), is attenuated in the presence of the solvent (*o*-DCB). Determination of the free energies allowed the estimation of the relative abundances of the *cis-anti-cis* and *cis-syn-cis* hexa-adducts, confirming that the former predominates under the experimental conditions.

## Experimental Section

**Synthesis of  $C_{60}$ -TM.**  $C_{60}$ -TM was synthesized following a procedure previously reported.<sup>[17]</sup>

**Synthesis of compounds 2 and 3.** Penta-adduct 2 and hexa-adduct 3 were synthesized by reacting  $C_{60}$ -TM (50 mg, 0.04 mmol) with methyl glycine ester hydrochloride (20 mg, 0.16 mmol) in the presence of diacetoxyiodobenzene (39 mg, 0.12 mmol) and sodium carbonate decahydrated (37 mg, 0.13 mmol) in *o*-DCB (10 mL), under sonication at room temperature and covered from light. After 30 min the solution

turned orange and compound 2 was the major product, however after 3 h the solution turned yellow and compound 3 was the main product as monitored by TLC using DCM:EA 30:1 mixture, as the eluent. After column chromatography purification compounds 2 and 3 were characterized by MALDI-TOF-MS and NMR spectroscopy.

**Synthesis of compound 7.** Hexa-adduct 7 was synthesized by reacting  $C_{60}$ -TM (50 mg, 0.04 mmol) with 2-picolylamine (17 mg, 0.16 mmol) and 2-pyridinecarbaldehyde (17 mg, 0.16 mmol) in *o*-DCB (10 mL), under reflux. After 30 min the solution turned yellow and compound 7 was the only product as monitored by TLC using  $CHCl_3$ :MeOH 15:1 mixture, as the eluent. After column chromatography purification compound 7 was characterized by MALDI-TOF-MS and NMR spectroscopy.

**Computational details.** The theoretical study of the 1,3-dipolar cycloaddition reactions of azomethine ylides has been performed by DFT methodology using ADF2016 code.<sup>[21, 22]</sup> An exhaustive exploration of the potential products was performed including the relative arrangements of the malonates with respect to pyrrolidine groups (See Figure 1 and Table S1). The exchange-correlation GGA density functional of Becke and Perdew (BP86) were employed to calculate all the minima.<sup>[23, 24]</sup> Relativistic corrections were included by means of the ZORA (the Zeroth Order Regular Approximation) formalism.<sup>[25-27]</sup> Dispersion corrections were also incorporated (D3 method by Grimme)<sup>[28]</sup> Solvent effects were included via the conductor-like screening model (COSMO) using Solvent Excluded Surface (SES).<sup>[29, 30]</sup> Slater Basis sets of TZP quality were used to describe the valence electrons of H, C, N and O. Frozen cores of C, N and O were described by means of single Slater functions.

## Acknowledgements

L.E. thanks the US National Science Foundation (NSF) for generous support of this work under the NSF-PREM program (DMR 1205302) and the CHE-1408865. The Robert A. Welch Foundation is also gratefully acknowledged for an endowed chair to L.E. (Grant AH-0033). This work was also supported by the Spanish Ministerio de Ciencia e Innovación (Project No. CTQ2014-52774-P) and the Generalitat de Catalunya (2014SGR-199 and XRQTC). J.M.P. thanks the ICREA foundation for an ICREA ACADEMIA award. M.M.O. and A.A. thank Beamline 11.3.1 at the Advanced Light Source synchrotron facility. The Advanced Light Source is supported by the Director, Office of Science, Office of Basic Energy Sciences, of the U.S. Department of Energy under Contract No. DE-AC02-05CH11231.

**Keywords:** fullerenes • hexa-adducts • *trans*-1 • regiochemistry • stereochemistry

## References

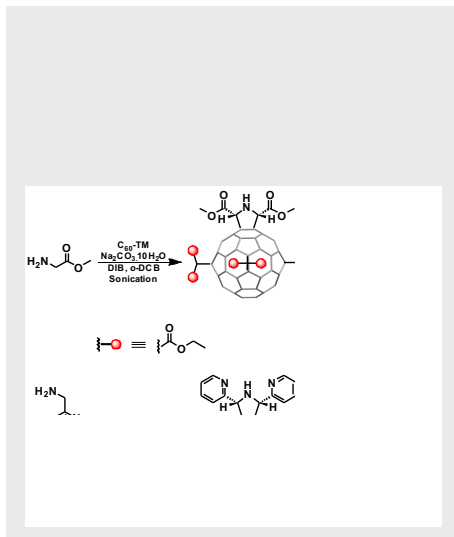
- [1] A. Hirsch, in *Fullerenes and Related Structures*, Vol. 199, Springer Berlin Heidelberg, 1999, pp. 1.
- [2] L. Pasimeni, A. Hirsch, I. Lamparth, A. Herzog, M. Maggini, M. Prato, C. Corvaja, G. Scorrano, *J. Am. Chem. Soc.* **1997**, *119*, 12896.
- [3] P. W. Fowler, *J. Chem. Soc., Faraday Trans.* **1995**, *91*, 2241.

- [4] U. Ortiz-Méndez, in *Handbook of Less-Common Nanostructures*, CRC Press, **2012**, pp. 623.
- [5] K. Kordatos, S. Bosi, T. Da Ros, A. Zambon, V. Lucchini, M. Prato, *J. Org. Chem.* **2001**, *66*, 2802.
- [6] S. Bosi, T. Da Ros, G. Spalluto, J. Balzarini, M. Prato, *Bioorg. Med. Chem. Lett.* **2003**, *13*, 4437.
- [7] Q. Lu, D. I. Schuster, S. R. Wilson, *J. Org. Chem.* **1996**, *61*, 4764.
- [8] L. Isaacs, R. F. Haldimann, F. Diederich, *Angew. Chem. Int. Ed. Engl.* **1994**, *33*, 2339.
- [9] B. Kräutler, T. Müller, J. Maynollo, K. Gruber, C. Kratky, P. Ochsenbein, D. Schwarzenbach, H.-B. Bürgi, *Angew. Chem. Int. Ed. Engl.* **1996**, *35*, 1204.
- [10] M. R. Cerón, M. Izquierdo, Y. Pi, S. L. Atehortúa, L. Echegoyen, *Chem. Eur. J.* **2015**, *21*, 7881.
- [11] M. J. van Eis, R. J. Alvarado, L. Echegoyen, P. Seiler, F. Diederich, *Chem. Commun.* **2000**, 1859.
- [12] S. Zhang, O. Lukoyanova, L. Echegoyen, *Chem. Eur. J.* **2006**, *12*, 2846.
- [13] E. E. Maroto, A. de Cózar, S. Filippone, Á. Martín-Domenech, M. Suarez, F. P. Cossío, N. Martín, *Angew. Chem. Int. Ed. Engl.* **2011**, *50*, 6060.
- [14] E. E. Maroto, S. Filippone, A. Martín-Domenech, M. Suarez, N. Martín, *J. Am. Chem. Soc.* **2012**, *134*, 12936.
- [15] E. E. Maroto, M. Izquierdo, S. Reboledo, J. Marco-Martínez, S. Filippone, N. Martín, *Acc. Chem. Res.* **2014**, *47*, 2660.
- [16] V. A. Ioutsi, A. A. Zadorin, P. A. Khavrel, N. M. Belov, N. S. Ovchinnikova, A. A. Goryunkov, O. N. Kharybin, E. N. Nikolaev, M. A. Yurovskaya, L. N. Sidorov, *Tetrahedron.* **2010**, *66*, 3037.
- [17] R. Schwenninger, T. Müller, B. Kräutler, *J. Am. Chem. Soc.* **1997**, *119*, 9317.
- [18] H. Hofmeier, U. S. Schubert, *Chem. Soc. Rev.* **2004**, *33*, 373.
- [19] A. D'Aléo, E. Cecchetto, L. De Cola, R. Williams, *Sensors.* **2009**, *9*, 3604.
- [20] G. Pandey, P. Banerjee, S. R. Gadre, *Chem. Rev.* **2006**, *106*, 4484.
- [21] C. Fonseca Guerra, J. G. Snijders, G. te Velde, E. J. Baerends, *Theor. Chem. Acc.* **1998**, *99*, 391.
- [22] G. te Velde, F. M. Bickelhaupt, E. J. Baerends, C. Fonseca Guerra, S. J. A. van Gisbergen, J. G. Snijders, T. Ziegler, *J. Comput. Chem.* **2001**, *22*, 931.
- [23] A. D. Becke, *Phys. Rev. A.* **1988**, *38*, 3098.
- [24] A. D. Becke, *J. Chem. Phys.* **1993**, *98*, 5648.
- [25] E. v. Lenthe, E. J. Baerends, J. G. Snijders, *J. Chem. Phys.* **1993**, *99*, 4597.
- [26] E. v. Lenthe, E. J. Baerends, J. G. Snijders, *J. Chem. Phys.* **1994**, *101*, 9783.
- [27] E. v. Lenthe, A. Ehlers, E.-J. Baerends, *J. Chem. Phys.* **1999**, *110*, 8943.
- [28] S. Grimme, J. Antony, S. Ehrlich, H. Krieg, *J. Chem. Phys.* **2010**, *132*, 154104.
- [29] A. Klamt, *J. Phys. Chem.* **1995**, *99*, 2224.
- [30] A. Klamt, V. Jonas, T. Bürger, J. C. W. Lohrenz, *J. Phys. Chem. A.* **1998**, *102*, 5074..

## Entry for the Table of Contents

## FULL PAPER

We report a totally unanticipated regio- and stereo-selective *bis*-1,3-dipolar cycloaddition to  $C_{60}$ -(*e,e,e,e*)-*tetra*-malonate that leads to the formation of a pure  $C_{2h}$ -symmetric *trans*-1-(*bis*-pyrrolidine)-*tetra*-malonate *hexa*-adduct of  $C_{60}$ .



Author(s), Luis Echegoyen,\* Josep M. Poblet,\* Marilyn M. Olmstead.\*

**Page No. – Page No.**  
**Unusual  $C_{2h}$ -symmetric *trans*-1-(*bis*-pyrrolidine)-*tetra*-malonate *hexa*-adducts of  $C_{60}$ . The unexpected regio- and stereo-control mediated by malonate-pyrrolidine interaction.**